Appears in the Proceedings of IEEE WCNC'07, March 2007.

A Three-Dimensional MIMO Mobile-to-Mobile Channel Model

Alenka G. Zajić and Gordon L. Stüber
School of Electrical and Computer Engineering
Georgia Institute of Technology, Atlanta, GA 30332 USA

***Abstract*— A three-dimensional (3-D) geometrical propagation model for multi-input-multi-output (MIMO) mobile-to-mobile (M-to-M) communications is proposed. Based on the geometrical model, a 3-D reference model for MIMO M-to-M multipath fading channels is proposed. From the reference model, a closed-form joint space-time correlation function is derived for a 3-D non-isotropic scattering environment and it is shown that many existing correlation functions are special cases of the derived space-time correlation function.**

I. Introduction

Mobile-to-mobile (M-to-M) communications play an important role in mobile ad-hoc wireless networks, intelligent transportation systems, and relay-based cellular networks. M-to-M communication systems are equipped with low elevation antennas and have both the transmitter ($\mathrm{T_x}$) and receiver ($\mathrm{R_x}$) in motion. To successfully design M-to-M systems, it is necessary to have a detailed knowledge of the multipath fading channel and its statistical properties. Early studies of single-input-single-output (SISO) M-to-M Rayleigh fading channels are reported in [1], [2]. They showed that the received envelope of M-to-M channels is Rayleigh faded under non line-of-sight conditions, but the statistical properties differ from fixed-to-mobile (F-to-M) channels.They also proposed a reference model for SISO M-to-M Rayleigh fading channels. Simulation models for SISO M-to-M channels have been proposed in [3]-[5]. Recently, the reference models for narrow-band multiple-input-multiple-output (MIMO) M-to-M channels have been proposed in [6], [7]. Simulation models for MIMO M-to-M channels have been proposed in [8], [9].

All previously reported models assume that the field incident on the ($\mathrm{T_x}$) or ($\mathrm{R_x}$) antenna is composed of a number of waves travelling only in the *horizontal* plane. This assumption is acceptable only for certain environments, e.g., rural areas. However, it does not seem appropriate for urban environment in which the ($\mathrm{T_x}$) and ($\mathrm{R_x}$) antenna arrays are often located in close proximity to and lower than surrounding buildings. Scattered waves may propagate by diffraction from the tops of buildings down to the street, and thus not necessarily travel horizontally. Hence, this paper proposes a three-dimensional (3-D) reference model for MIMO M-to-M multipath fading channels. To describe our 3-D reference model, we first introduce a 3-D geometrical model for MIMO M-to-M channels, referred to as a "two-cylinder" model. This model is extension of the one-cylinder model for F-to-M channels proposed in [10], [11]. By taking into account local scattering around both the $\mathrm{T_x}$ and $\mathrm{R_x}$ and by including mobility of both the $\mathrm{T_x}$ and $\mathrm{R_x}$, we obtain our two-cylinder model. From the 3-D reference model, we derive a closed-form joint space-time correlation function for a 3-D non-isotropic scattering environment. Furthermore, we show that many existing correlation functions are special cases of our 3-D MIMO M-to-M space-time correlation function. Finally, we present some simulation results to verify theoretical derivations.

The remainder of the paper is organized as follows. Section II introduces a geometrical two-cylinder model. Section III presents a 3-D reference model for MIMO M-to-M channels. Section IV derives the closed-form joint space-time correlation function for 3-D non-isotropic scattering. Section V presents some simulation results to verify theoretical derivations. Finally, Section VI provides some concluding remarks.

II. A Geometrical Two-Cylinder Model

In this section, we introduce a 3-D geometrical model for MIMO M-to-M channels, called a two-cylinder model. We consider a narrow-band MIMO communication system with L_t transmit and L_r receive omnidirectional antenna elements. It is assumed that both the $\mathrm{T_x}$ and $\mathrm{R_x}$ are in motion and equipped with low elevation antennas. The radio propagation environment is characterized by 3-D scattering with non-line-of-sight (NLoS) propagation conditions between the $\mathrm{T_x}$ and $\mathrm{R_x}$.

The two-cylinder model is an extension of the one-cylinder model for F-to-M channels proposed in [10], [11]. By taking into account local scattering around both the $\mathrm{T_x}$ and $\mathrm{R_x}$ and by including mobility of both the $\mathrm{T_x}$ and $\mathrm{R_x}$, we obtain our two-cylinder model.

Fig. 1 shows the two-cylinder model for a MIMO M-to-M channel with $L_t = L_r = 2$ antenna elements. The two-cylinder model defines two cylinders, one around the $\mathrm{T_x}$ and another around the $\mathrm{R_x}$, as shown in Fig. 1. Around the transmitter, M fixed omnidirectional scatterers lie on a surface of a cylinder of radius R_t, and the m^{th} transmit scatterer is denoted by $S_T^{(m)}$. Similarly, around the receiver, N fixed omnidirectional scatterers lie on the surface of a cylinder of radius R_r, and

0
Prepared through collaborative participation in the Collaborative Technology Alliance for Communications & Networks sponsored by the U.S. Army Research Laboratory under Cooperative Agreement DAAD19-01-2-0011. The U.S. Government is authorized to reproduce and distribute reprints for Government purposes notwithstanding any copyright notation thereon.

the n^{th} receive scatterer is denoted by $S_R^{(n)}$. The distance between the centers of the $\mathrm{T_x}$ and $\mathrm{R_x}$ cylinders is D. It is assumed that the radii R_t and R_r are much smaller than the distance D, i.e., $\max\{R_t, R_r\} \ll D$. The spacing between antenna elements at the $\mathrm{T_x}$ and $\mathrm{R_x}$ is denoted by d_T and d_R, respectively. It is assumed that d_T and d_R are much smaller than the radii R_t and R_r, i.e., $\max\{d_T, d_R\} \ll \min\{R_t, R_r\}$. Angles θ_T and θ_R describe the orientation of the $\mathrm{T_x}$ and $\mathrm{R_x}$ antenna array in the x-y plane, respectively, relative to the x-axis. Similarly, angles ψ_T and ψ_R describe the elevation of the $\mathrm{T_x}$'s antenna array and the $\mathrm{R_x}$'s antenna array relative to the x-y plane, respectively. The $\mathrm{T_x}$ and $\mathrm{R_x}$ are moving with speeds v_T and v_R in directions described by angles γ_T and γ_R, respectively. The symbols $\alpha_T^{(m)}$ and $\alpha_R^{(n)}$ denote the azimuth angle of departure (AAoD) and the azimuth angle of arrival (AAoA), respectively. Similarly, the symbols $\beta_T^{(m)}$ and $\beta_R^{(n)}$ denote the elevation angle of departure (EAoD) and the elevation angle of arrival (EAoA), respectively. Finally, the symbols ϵ_{pm}, ϵ_{mn}, and ϵ_{nq} denote distances $A_T^{(p)}$–$S_T^{(m)}$, $S_T^{(m)}$–$S_R^{(n)}$, and $S_R^{(n)}$–$A_R^{(q)}$, respectively, as shown in Fig. 1.

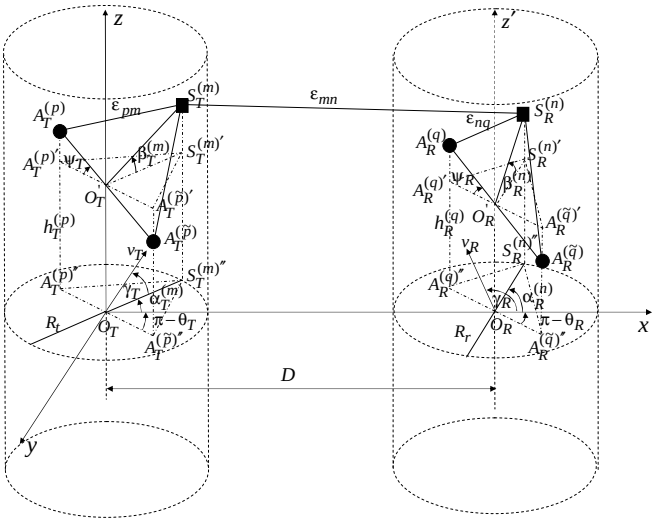

Fig. 1. The two-cylinder model for MIMO M-to-M channel with $L_t = L_r = 2$ antenna elements.

III. A 3-D Reference Model for MIMO Mobile-to-Mobile Channels

In this section, we derive a reference model for MIMO M-to-M multipath fading channels. The starting point is the two-cylinder model shown in Fig. 1. From the two-cylinder model, we observe that the waves from the $\mathrm{T_x}$ antenna elements first arrive at the scatterers located on the $\mathrm{T_x}$ cylinder. Considering these fixed scatterers as "virtual base-stations" (VBS), the communication link from each VBS to the $\mathrm{R_x}$ is modelled as a 3-D F-to-M link. The signals from each VBS arrive at the $\mathrm{R_x}$ antenna from all directions and with equal power due to 3-D scattering around the $\mathrm{R_x}$.

The MIMO channel is described by an $L_r \times L_t$ matrix $\mathbf{H}(t) = [h_{ij}(t)]_{L_r \times L_t}$ of complex low-pass faded envelopes. In the 3-D reference model, the number of local scatterers around the $\mathrm{T_x}$ and $\mathrm{R_x}$ is infinite. Consequently, the received complex faded envelope of the link $A_T^{(p)} - A_R^{(q)}$ is

$$h_{pq}(t) = \lim_{M,N\to\infty} \sqrt{\frac{1}{MN}} \sum_{m=1}^{M} \sum_{n=1}^{N} e^{-j\frac{2\pi}{\lambda}(\epsilon_{pm}+\epsilon_{mn}+\epsilon_{nq})+j\phi_{mn}} e^{j2\pi t[f_{T\max}\cos(\alpha_T^{(m)}-\gamma_T)\cos\beta_T^{(m)} + f_{R\max}\cos(\alpha_R^{(n)}-\gamma_R)\cos\beta_R^{(n)}]}, \quad (1)$$

where $f_{T\max} = v_T/\lambda$ and $f_{R\max} = v_R/\lambda$ are the maximum Doppler frequencies associated with the $\mathrm{T_x}$ and $\mathrm{R_x}$, respectively, and λ is the carrier wavelength. It is assumed that the angles of departures (AAoDs and EAoDs) and the angles of arrivals (AAoAs and EAoAs) are random variables, and that the angles of departure are independent from the angles of arrival. Additionally, it is assumed that the phases ϕ_{mn} are random variables uniformly distributed on the interval $[-\pi, \pi)$ and independent form the angles of departures and the angles of arrivals.

The distances ϵ_{pm}, ϵ_{mn}, and ϵ_{nq} can be expressed as functions of the random variables $\alpha_T^{(m)}$, $\alpha_R^{(n)}$, $\beta_T^{(m)}$, and $\beta_R^{(n)}$ as follows:

$$\epsilon_{pm} \approx R_t - \frac{d_T}{2}\sin\psi_T \sin\beta_T^{(m)} - \frac{d_T}{2}\cos\psi_T\cos\beta_T^{(m)}\left(\cos\theta_T\cos\alpha_T^{(m)} + \sin\theta_T\sin\alpha_T^{(m)}\right), \quad (2)$$

$$\epsilon_{nq} \approx R_r - \frac{d_R}{2}\sin\psi_R \sin\beta_R^{(n)} - \frac{d_R}{2}\cos\psi_R\cos\beta_R^{(n)}\left(\cos\theta_R\cos\alpha_R^{(n)} + \sin\theta_R\sin\alpha_R^{(n)}\right), \quad (3)$$

$$\epsilon_{mn} \approx D. \quad (4)$$

Derivations of expressions (2) - (4) are omitted for brevity.

Using (2) - (4), the complex faded envelope of the link $A_T^{(p)} - A_R^{(q)}$ can be rewritten as

$$h_{pq}(t) = \lim_{M,N\to\infty} \frac{1}{\sqrt{MN}} \sum_{m,n=1}^{M,N} a_{p,m} b_{n,q} e^{j\phi_{mn}+j\phi_0} e^{j2\pi t[f_{T\max}\cos(\alpha_T^{(m)}-\gamma_T)\cos\beta_T^{(m)} + f_{R\max}\cos(\alpha_R^{(n)}-\gamma_R)\cos\beta_R^{(n)}]}, \quad (5)$$

where $\phi_0 = -2\pi\left(R_t + R_r + D\right)/\lambda$ and parameters $a_{p,m}$ and $b_{n,q}$ are defined as

$$a_{p,m} = e^{j\frac{\pi}{\lambda}d_T\sin\psi_T\sin\beta_T^{(m)}} e^{j\frac{\pi}{\lambda}d_T\cos\psi_T\cos\beta_T^{(m)}(\cos\theta_T\cos\alpha_T^{(m)}+\sin\theta_T\sin\alpha_T^{(m)})}, \quad (6)$$

$$b_{n,q} = e^{j\frac{\pi}{\lambda}d_R\sin\psi_R\sin\beta_R^{(n)}} e^{j\frac{\pi}{\lambda}d_R\cos\psi_R\cos\beta_R^{(n)}(\cos\theta_R\cos\alpha_R^{(n)}+\sin\theta_R\sin\alpha_R^{(n)})}. \quad (7)$$

Note that the constant phase ϕ_0 can be set to zero without loss of generality, because it does not affect statistical properties of the model.

IV. Space-Time Correlation Function of the 3-D Reference Model

Assuming a 3-D non-isotropic scattering environment, we now derive the space-time correlation function of the complex faded envelope described in (5). The normalized space-time correlation function between two complex faded envelopes $h_{pq}(t)$ and $h_{\tilde{p}\tilde{q}}(t)$ is defined as

$$R_{pq,\tilde{p}\tilde{q}}[d_T, d_R, \tau] = \frac{\mathrm{E}\left[h_{pq}(t) h^*_{\tilde{p}\tilde{q}}(t+\tau)\right]}{\sqrt{\mathrm{E}[|h_{pq}(t)|^2]\mathrm{E}[|h_{\tilde{p}\tilde{q}}(t)|^2]}}, \quad (8)$$

where $(\ \cdot\ )^*$ denotes complex conjugate operation, $\mathrm{E}[\ \cdot\ ]$ is the statistical expectation operator, $p, \tilde{p} \in \{1, \ldots, L_t\}$, and $q, \tilde{q} \in \{1, \ldots, L_r\}$. Using (5) and (8), the space-time correlation function can be written as

$$R_{pq,\tilde{p}\tilde{q}}[d_T, d_R, \tau] = \lim_{M,N\to\infty} \frac{1}{MN} \sum_{m,n=1}^{M,N} \mathrm{E}\Big[a_{p,m} b_{n,q} a^*_{\tilde{p},m} b^*_{n,\tilde{q}} \quad (9)$$
$$e^{-j2\pi\tau \ \ f_{T\max}\cos(\alpha_T^{(m)}-\gamma_T)\cos\beta_T^{(m)} + f_{R\max}\cos(\alpha_R^{(n)}-\gamma_R)\cos\beta_R^{(n)}} \Big].$$

Since the number of local scatterers in the reference model described in Section III is infinite, the discrete AAoDs, $\alpha_T^{(m)}$, EAoDs, $\beta_T^{(m)}$, AAoAs, $\alpha_R^{(n)}$, and EAoAs, $\beta_R^{(n)}$, can be replaced with continuous random variables α_T, β_T, α_R, and β_R with probability density functions (pdf) $f(\alpha_T)$, $f(\beta_T)$, $f(\alpha_R)$, and $f(\beta_R)$, respectively. Hence, (9) can be rewritten as

$$R_{pq,\tilde{p}\tilde{q}}[d_T, d_R, \tau] = \int_{-\beta_{R_m}}^{\beta_{R_m}} \int_{-\beta_{T_m}}^{\beta_{T_m}} \int_{-\pi}^{\pi} \int_{-\pi}^{\pi} f(\alpha_T) f(\beta_T) f(\alpha_R) f(\beta_R)$$
$$e^{-j2\pi\tau f_{T\max}\cos(\alpha_T-\gamma_T)\cos\beta_T + j\frac{2\pi}{\lambda} d_T \sin\psi_T \sin\beta_T} \quad (10)$$
$$e^{j\frac{2\pi}{\lambda} d_T \cos\psi_T \cos\beta_T \cos\theta_T \cos\alpha_T + j\frac{2\pi}{\lambda} d_T \cos\psi_T \cos\beta_T \sin\theta_T \sin\alpha_T}$$
$$e^{-j2\pi\tau f_{R\max}\cos(\alpha_R-\gamma_R)\cos\beta_R + j\frac{2\pi}{\lambda} d_R \sin\psi_R \sin\beta_R}$$
$$e^{j\frac{2\pi}{\lambda} d_R \cos\psi_R \cos\beta_R(\cos\theta_R \cos\alpha_R + \sin\theta_R \sin\alpha_R)} d\alpha_T d\beta_T d\alpha_R d\beta_R,$$

where β_{T_m} and β_{R_m} are the maximum elevation angles of the scatterers around the $\mathrm{T_x}$ and $\mathrm{R_x}$, respectively.

Several different scatterer distributions, such as uniform, Gaussian, Laplacian, and von Mises, are used in prior work to characterize the continuous random variables α_T and α_R. In this paper, we use the von Mises pdf because it approximates many of the previously mentioned distributions and leads to closed-form solutions for many useful situations. The von Mises pdf is defined as [12]

$$f(\theta) = \frac{1}{2\pi I_0(k)} \exp\left[k\cos(\theta-\mu)\right], \quad (11)$$

where $\theta \in [-\pi, \pi)$, $I_0(\ \cdot\ )$ is the zeroth-order modified Bessel function of the first kind, $\mu \in [-\pi, \pi)$ is the mean angle at which the scatterers are distributed in the x - y plane, and k controls the spread of scatterers around the mean. To characterize the continuous random variables β_T and β_R, we use the pdf [11]

$$f(\varphi) = \begin{cases} \frac{\pi}{4|\varphi_m|}\cos\left(\frac{\pi}{2}\frac{\varphi}{\varphi_m}\right) & , \ |\varphi| \le |\varphi_m| \le \frac{\pi}{2} \\ 0 & , \ \text{otherwise} \end{cases}, \quad (12)$$

where φ_m is the maximum elevation angle and takes values in the range $10^\circ \le |\varphi_m| \le 20^\circ$ [13].

By grouping the terms in (10) into those containing α_T and β_T and those containing α_R and β_R, the integrals in (10) reduce to the product of two double integrals, because the random variables α_T and β_T are independent from the random variables α_R and β_R. By denoting the von Mises pdf for the $\mathrm{T_x}$ and $\mathrm{R_x}$ azimuth angles as $f(\alpha_T) = \exp\left[k_T\cos(\alpha_T-\mu_T)\right]/(2\pi I_0(k_T))$ and $f(\alpha_R) = \exp\left[k_R\cos(\alpha_R-\mu_R)\right]/(2\pi I_0(k_R))$, respectively, and by denoting the pdf for the $\mathrm{T_x}$ and $\mathrm{R_x}$ elevation angles as $f(\beta_T) = \pi\cos(\pi\beta_T/(2\beta_{T_m}))/(4|\beta_{T_m}|)$ and $f(\beta_R) = \pi\cos(\pi\beta_R/(2\beta_{R_m}))/(4|\beta_{R_m}|)$, respectively, the space-time correlation function becomes

$$R_{pq,\tilde{p}\tilde{q}}[d_T, d_R, \tau] = R^T_{p,\tilde{p}}[d_T, \tau] R^R_{q,\tilde{q}}[d_R, \tau] = \quad (13)$$
$$\int_{-\beta_{T_m}}^{\beta_{T_m}} \int_{-\pi}^{\pi} g(\alpha_T, \beta_T) d\alpha_T d\beta_T \int_{-\beta_{R_m}}^{\beta_{R_m}} \int_{-\pi}^{\pi} g(\alpha_R, \beta_R) d\alpha_R d\beta_R,$$

where $g(\alpha_T, \beta_T)$ and $g(\alpha_R, \beta_R)$ are defined as

$$g(\alpha_T, \beta_T) = \frac{\pi}{4|\beta_{T_m}|}\cos\left(\frac{\pi}{2}\frac{\beta_T}{\beta_{T_m}}\right)\frac{\exp\left\{k_T\cos(\alpha_T-\mu_T)\right\}}{2\pi I_0(k_T)}$$
$$e^{-j2\pi\tau f_{T\max}\cos(\alpha_T-\gamma_T)\cos\beta_T + j\frac{2\pi}{\lambda} d_T \sin\psi_T \sin\beta_T}$$
$$e^{j\frac{2\pi}{\lambda} d_T \cos\psi_T \cos\beta_T[\cos\theta_T\cos\alpha_T + \sin\theta_T\sin\alpha_T]}, \quad (14)$$

$$g(\alpha_R, \beta_R) = \frac{\pi}{4|\beta_{R_m}|}\cos\left(\frac{\pi}{2}\frac{\beta_R}{\beta_{R_m}}\right)\frac{\exp\left\{k_R\cos(\alpha_R-\mu_R)\right\}}{2\pi I_0(k_R)}$$
$$e^{-j2\pi\tau f_{R\max}\cos(\alpha_R-\gamma_R)\cos\beta_R + j\frac{2\pi}{\lambda} d_R \sin\psi_R \sin\beta_R}$$
$$e^{j\frac{2\pi}{\lambda} d_R \cos\psi_R \cos\beta_R[\cos\theta_R\cos\alpha_R + \sin\theta_R\sin\alpha_R]}, \quad (15)$$

respectively. Using trigonometric transformations and the equality $\int_{-\pi}^{\pi} \exp\left\{a\sin(c) + b\cos(c)\right\} dc = 2\pi I_0(\sqrt{a^2+b^2})$ [14, eq. 3.338-4], the space-time correlation function becomes

$$R_{pq,\tilde{p}\tilde{q}}[d_T, d_R, \tau] = R^T_{p,\tilde{p}}[d_T, \tau] R^R_{q,\tilde{q}}[d_R, \tau] = \quad (16)$$
$$\int_{-\beta_{T_m}}^{\beta_{T_m}} \pi\cos\left(\frac{\pi}{2}\frac{\beta_T}{\beta_{T_m}}\right)\frac{e^{j\frac{2\pi}{\lambda} d_T \sin\psi_T \sin\beta_T}}{4|\beta_{T_m}|}\frac{I_0(\sqrt{x^2+y^2}\cos\beta_T)}{I_0(k_T)} d\beta_T$$
$$\int_{-\beta_{R_m}}^{\beta_{R_m}} \pi\cos\left(\frac{\pi}{2}\frac{\beta_R}{\beta_{R_m}}\right)\frac{e^{j\frac{2\pi}{\lambda} d_R \sin\psi_R \sin\beta_R}}{4|\beta_{R_m}|}\frac{I_0(\sqrt{z^2+w^2}\cos\beta_R)}{I_0(k_R)} d\beta_R,$$

where parameters x, y, z, and w are

$$x = j2\pi d_{T_x}/\lambda - j2\pi\tau f_{T\max}\cos\gamma_T + k_T\cos\mu_T/\cos\beta_T,$$
$$y = j2\pi d_{T_y}/\lambda - j2\pi\tau f_{T\max}\sin\gamma_T + k_T\sin\mu_T/\cos\beta_T,$$
$$z = j2\pi d_{R_x}/\lambda - j2\pi\tau f_{R\max}\cos\gamma_R + k_R\cos\mu_R/\cos\beta_R,$$
$$w = j2\pi d_{R_y}/\lambda - j2\pi\tau f_{R\max}\sin\gamma_R + k_R\sin\mu_R/\cos\beta_R,$$

and where $d_{T_x} = d_T\cos\theta_T\cos\psi_T$, $d_{T_y} = d_T\sin\theta_T\cos\psi_T$, $d_{R_x} = d_R\cos\theta_R\cos\psi_R$, and $d_{R_y} = d_R\sin\theta_R\cos\psi_R$. To obtain the space-time correlation function for the 3-D MIMO M-to-M system, the integrals in (16) have to be evaluated numerically, because they do not have closed-form solutions. Since β_T and β_R are small angles, i.e., $|\beta_T|, |\beta_R| \le 20^\circ$, using approximations $\cos\beta_T, \cos\beta_R \approx 1$, $\sin\beta_T \approx \beta_T$, and

$\sin\beta_R \approx \beta_R$, the space-time correlation function can be approximated as

$$R_{pq,\tilde{p}\tilde{q}}[d_T, d_R, \tau] = R^T_{p,\tilde{p}}[d_T, \tau] R^R_{q,\tilde{q}}[d_R, \tau] \approx \quad (17)$$
$$\frac{I_0(\sqrt{x_1^2+y_1^2})}{I_0(k_T)} \int_{-\beta_{T_m}}^{\beta_{T_m}} \frac{\pi}{4|\beta_{T_m}|} \cos\left(\frac{\pi}{2}\frac{\beta_T}{\beta_{T_m}}\right) e^{j\frac{2\pi}{\lambda} d_T \sin\psi_T \beta_T} d\beta_T$$
$$\frac{I_0(\sqrt{z_1^2+w_1^2})}{I_0(k_R)} \int_{-\beta_{R_m}}^{\beta_{R_m}} \frac{\pi}{4|\beta_{R_m}|} \cos\left(\frac{\pi}{2}\frac{\beta_R}{\beta_{R_m}}\right) e^{j\frac{2\pi}{\lambda} d_R \sin\psi_R \beta_R} d\beta_R,$$

where parameters x_1, y_1, z_1, and w_1 are

$$\begin{aligned} x_1 &= j2\pi d_{T_x}/\lambda - j2\pi\tau f_{T\max}\cos\gamma_T + k_T\cos\mu_T, \\ y_1 &= j2\pi d_{T_y}/\lambda - j2\pi\tau f_{T\max}\sin\gamma_T + k_T\sin\mu_T, \\ z_1 &= j2\pi d_{R_x}/\lambda - j2\pi\tau f_{R\max}\cos\gamma_R + k_R\cos\mu_R, \\ w_1 &= j2\pi d_{R_y}/\lambda - j2\pi\tau f_{R\max}\sin\gamma_R + k_R\sin\mu_R. \end{aligned} \quad (18)$$

Finally, solving the integrals in (17), the space-time correlation function becomes

$$R_{pq,\tilde{p}\tilde{q}}[d_T, d_R, \tau] \approx \frac{I_0(\sqrt{x_1^2+y_1^2})\cos\left(\frac{2\pi}{\lambda}\beta_{T_m} d_T \sin\psi_T\right)}{I_0(k_T)\left[1-\left(\frac{4\beta_{T_m} d_T \sin\psi_T}{\lambda}\right)^2\right]}$$
$$\frac{I_0(\sqrt{w_1^2+z_1^2})\cos\left(\frac{2\pi}{\lambda}\beta_{R_m} d_R \sin\psi_R\right)}{I_0(k_R)\left[1-\left(\frac{4\beta_{R_m} d_R \sin\psi_R}{\lambda}\right)^2\right]}. \quad (19)$$

Many existing correlation functions are special cases of the 3-D MIMO M-to-M space-time correlation function in (19). The simplest special case of (19) is Clark's temporal correlation function $J_0(2\pi f_{R\max}\tau)$ [15], obtained for $k_R = \beta_{R_m} = 0$ (2-D isotropic scattering around $\mathrm{R_x}$), $f_{T\max} = k_T = 0$ (stationary $\mathrm{T_x}$, no scattering), and $d_T = d_R = 0$ (single-antenna $\mathrm{T_x}$ and $\mathrm{R_x}$), where $J_0(\cdot)$ is the first kind zeroth-order Bessel function. Expressions for other space-time correlation functions based on the one-ring model [16], [17] and based on the one-cylinder model [11], [18] can be similarly obtained. The temporal correlation function for M-to-M channels, assuming 2-D isotropic scattering, $J_0(2\pi f_{T\max}\tau)J_0(2\pi f_{R\max}\tau)$ [1], is obtained for $k_T = k_R = 0$, $d_T = d_R = 0$, and $\beta_{T_m} = \beta_{R_m} = 0$. Similarly, assuming 2-D isotropic scattering, the spatial correlation function for M-to-M channel $J_0(2\pi d_T/\lambda)J_0(2\pi d_R/\lambda)$ [19] is obtained for $k_T = k_R = 0$, $\beta_{T_m} = \beta_{R_m} = 0$ and $\tau = 0$. Finally, the space-time correlation function for M-to-M channels, assuming 2-D non-isotropic scattering, $I_0(\sqrt{x_1^2+y_1^2})I_0(\sqrt{z_1^2+w_1^2})/(I_0(k_T)I_0(k_R))$ [7] is obtained for $\beta_{T_m} = \beta_{R_m} = 0$.

V. Simulation Results

In this section, we present some simulation results to verify theoretical derivations. In all simulations, we use a normalized sampling period $f_{T\max}T_s = 0.01$ ($f_{T\max} = f_{R\max}$ are the maximum Doppler frequencies and T_s is the sampling period). Unless indicated otherwise, the number of transmit and receive antennas is set to $L_t = L_r = 2$.

To validate approximations used to obtain the space-time correlation function in (19), we compare it with the numerically obtained space-time correlation function in (16). Fig. 2 shows good agreement between the space-time correlation functions in (16) and (19). The parameters used to obtain curves in Fig. 2 are $d_T = d_R = 0.5\lambda$, $\beta_{Tm} = \beta_{Rm} = 20°$, $\theta_T = \theta_R = \pi/4$, $\psi_T = \psi_R = 2\pi/3$, $\gamma_T = 20°$, $\gamma_R = 40°$, and $k_T = k_R = 0$.

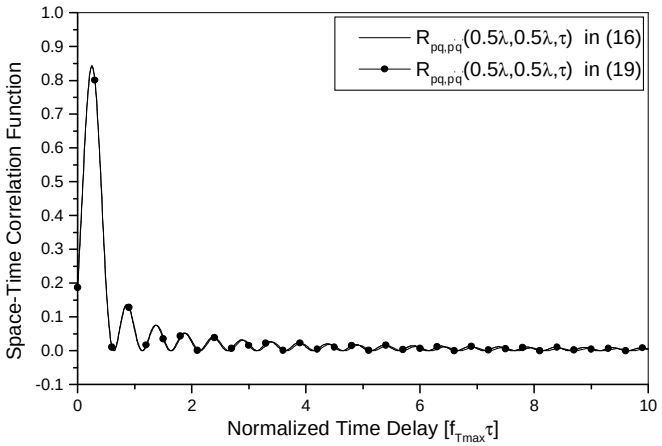

Fig. 2. Comparison of the normalized space-time correlation functions in (16) and (19).

The 2-D space-time correlation functions for M-to-M channels [6]-[9] suggest that two vertically placed antennas are completely correlated and no diversity gain is available. However, the 3-D space-time correlation function shows that vertically placed antennas can have small correlations and provide considerable diversity gain. To illustrate this, Fig. 3 shows the space-time correlation functions of two vertically spaced antennas at the $\mathrm{T_x}$ for several maximum elevation angles β_{T_m}. Other parameters used to obtain curves in Fig. 3 are $L_r = 1$, $\theta_T = \theta_R = 0$, $\psi_T = \pi/2$, $\psi_R = 0$, $\gamma_T = \gamma_R = 0$, and $k_T = k_R = 0$. As the maximum elevation angle β_{T_m} increases from $1°$ to $20°$, the correlation between the two antennas reduces dramatically.

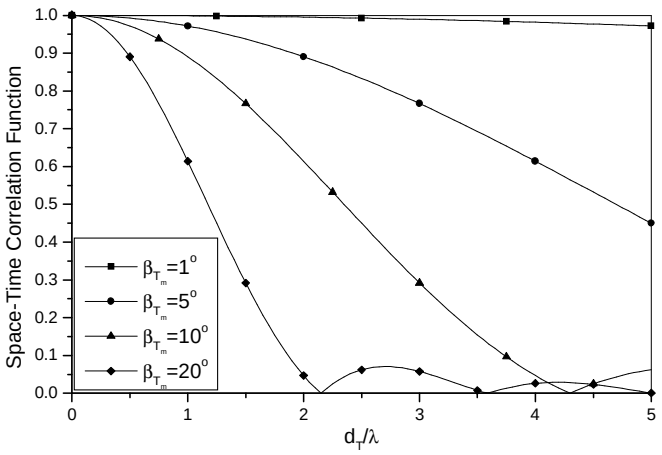

Fig. 3. The normalized space-time correlation functions of two vertically spaced antennas at the $\mathrm{T_x}$ for several maximum elevation angles β_{T_m}.

Finally, we illustrate how our 3-D space-time correlation function can be used to evaluate MIMO M-to-M capacity. The

ergodic channel capacity (in $\mathrm{bit/s/Hz}$) of a stochastic MIMO channel, under an average transmit power constraint, is given by [20]

$$\mathrm{E}[C(t)] = \mathrm{E}\left[\log_2 \det\left(\mathbf{I}_{L_r} + \frac{\rho}{L_t}\mathbf{H}(t)\mathbf{H}^H(t)\right)\right], \qquad (20)$$

where it is assumed that $L_t \geq L_r$, the transmitter has no channel knowledge, and the receiver has perfect channel knowledge. In (20), $\mathbf{H}(t) = [h_{ij}(t)]_{L_r \times L_t}$ is the $L_r \times L_t$ matrix of complex faded envelopes, $(\ \cdot\ )^H$ denotes the transpose conjugate operation, $\det(\ \cdot\ )$ denotes the matrix determinant, $\mathbf{I}_{L_r}$ is the $L_r \times L_r$ identity matrix, and ρ is the average signal-to-noise ratio (SNR). The channel matrix $\mathbf{H}$ can be generated as a product of the white channel matrix and the square root of desired correlation matrix [21], i.e.,

$$\mathbf{H} \quad = \quad (\mathbf{R}_T[d_T, 0])^{1/2}\mathbf{G}(\mathbf{R}_R[d_R, 0])^{T/2}, \qquad (21)$$

where $\mathbf{G}$ is an $L_t \times L_r$ stochastic matrix with complex Gaussian i.i.d. entries, $(\ \cdot\ )^{1/2}$ denotes the matrix square root operation, and $\mathbf{R}_T[d_T, 0]$ and $\mathbf{R}_R[d_R, 0]$ are the $L_t \times L_t$ transmit correlation matrix and the $L_r \times L_r$ receive correlation matrix, respectively. The elements of matrices $\mathbf{R}_T[d_T, 0]$ and $\mathbf{R}_R[d_R, 0]$ are obtained using (19). Fig. 4 shows the ergodic capacity against SNR, for several linear antenna arrays ($L_t = L_r = 2$, $L_t = L_r = 4$, and $L_t = L_r = 6$). Parameters used to obtain curves in Fig. 4 are $\theta_T = \theta_R = \pi/4$, $\psi_T = \psi_R = \pi/6$, $\gamma_T = 0$ and $\gamma_R = 20°$, $\beta_{Tm} = \beta_{Rm} = 15°$, $k_T = k_R = 5$, $\mu_T = \pi/2$, and $\mu_R = 3\pi/2$. The spacing between two adjacent antenna elements at the $\mathrm{T_x}$ and $\mathrm{R_x}$ is chosen to be 0.5λ.

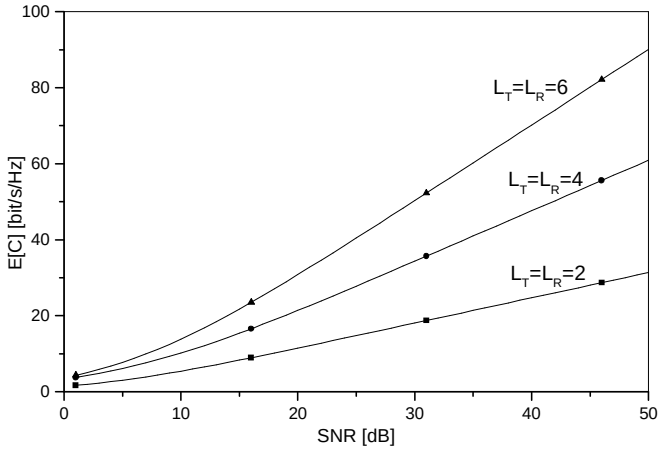

Fig. 4. Ergodic capacity obtained using the 3-D space-time correlation function in (19).

VI. Conclusions

In this paper, a two-cylinder geometrical propagation model is introduced. Based on this geometrical model, a 3-D reference model for MIMO M-to-M fading channels is proposed. From the reference model, a closed-form joint space-time correlation function for 3-D non-isotropic scattering environment is derived. It is shown that many existing correlation functions are special cases of our 3-D MIMO M-to-M space-time correlation function. Finally, some simulation results are presented to verify theoretical derivations.

Disclaimer

The views and conclusions contained in this document are those of the authors and should not be interpreted as representing the official policies, either expressed or implied, of the Army Research Laboratory or the U. S. Government.

References

[1] A.S. Akki and F. Haber, "A statistical model for mobile-to-mobile land communication channel," *IEEE Trans. on Veh. Tech.*, vol. 35, pp. 2–10, Feb. 1986.

[2] A.S. Akki, "Statistical properties of mobile-to-mobile land communication channels," *IEEE Trans. on Veh. Tech.*, vol. 43, pp. 826–831, Nov. 1994.

[3] R. Wang and D. Cox, "Channel modeling for ad hoc mobile wireless networks," *Proc. IEEE VTC'02.*, vol. 1, pp. 21–25, Birmingham, AL, May 2002.

[4] C.S. Patel, G.L. Stüber, and T. G. Pratt, "Simulation of Rayleigh-faded mobile-to-mobile communication channels," *IEEE Trans. on Commun.*, vol. 53, pp. 1876–1884, Nov. 2005.

[5] A.G. Zajić and G.L. Stüber, "A new simulation model for mobile-to-mobile Rayleigh fading channels," *Proc. IEEE WCNC'06*, vol. 3, pp. 1266–1270, Las Vegas, NE, USA, Apr. 2006.

[6] M. Pätzold, B.O. Hogstad, N. Youssef, and D. Kim, "A MIMO mobile-to-mobile channel model: Part I-the reference model," *Proc. IEEE PIMRC'05*, vol. 1, pp. 573–578, Berlin, Germany, Sept. 2005.

[7] A.G. Zajić and G.L. Stüber, "Space-Time Correlated MIMO Mobile-to-Mobile Channels," *Proc. IEEE PIMRC'06*, Helsinki, Finland, Sept. 2006.

[8] B.O. Hogstad, M. Pätzold, N. Youssef, and D. Kim, "A MIMO mobile-to-mobile channel model: Part II-the simulation model," *Proc. IEEE PIMRC'05*, vol. 1, pp. 562–567, Berlin, Germany, Sept. 2005.

[9] A.G. Zajić and G.L. Stüber, "Simulation Models for MIMO Mobile-to-Mobile Channels," *Proc. IEEE MILCOM'06*, Washington, D.C., USA, Oct. 2006.

[10] T. Aulin, "A modified model for the fading at a mobile radio channel," *IEEE Trans. on Veh. Tech.*, vol. VT–28, pp. 182–203, 1979.

[11] J.D. Parsons and A.M.D. Turkmani, "Characterisation of mobile radio signals: model description," *IEE Proc. I, Commun., Speach, and Vision*, vol. 138, pp. 549–556, Dec. 1991.

[12] A. Abdi, J.A. Barger, and M. Kaveh, "A parametric model for the distribution of the angle of arrival and the associated correlation function and power spectrum at the mobile station," *IEEE Trans. on Veh. Tech.*, vol. 51, pp. 425–434, May 2002.

[13] Y. Yamada, Y. Ebine, and N. Nakajima, "Base station/vehicular antenna design techniques employed in high capacity land mobile communications system," *Rev. Elec. Commun. Lab.*, NTT, pp. 115–121, 1987.

[14] I.S. Gradshteyn and I.M. Ryzhik, *Table of Integrals, Series, and Products* 5^{th} *ed.*. A. Jeffrey, Ed. San Diego CA: Academic, 1994.

[15] R.H. Clarke, "A statistical theory of mobile-radio reception," *Bell Syst. Tech. J.*, pp. 957–1000, July–Aug. 1968.

[16] D. Shiu, G.J. Foschini, M.J. Gans, and J.M. Khan, "Fading correlation and its effect on the capacity of multielement antenna systems," *IEEE Trans. on Commun.*, vol. 48, pp. 502–513, Mar. 2000.

[17] A. Abdi and M. Kaveh, "A space-time correlation model for multielement antenna systems in mobile fading channels,"*IEEE J. Select. Areas in Commun.*, vol. 20, pp. 550–560, Apr. 2002.

[18] S.Y. Leong, Y.R. Zheng, and C. Xiao, "Space-time fading correlation functions of a 3-D MIMO channel model," *Proc. IEEE WCNC'04*, vol. 2, pp. 1127–1132, Atlanta, GA, Mar. 2004.

[19] H. Kang, G.L. Stüber, T.G. Pratt, and M.A. Ingram, "Studies on the capacity of MIMO systems in mobile-to-mobile environment," *Proc. IEEE WCNC'04*, vol. 1, pp. 363–368, Atlanta, GA, Mar. 2004.

[20] I.E. Telatar, "Capacity of multiantenna Gaussian channels," *Eur. Trans. Telecommun.*, vol. 10, no. 6, pp. 585–595, Nov./Dec. 1999.

[21] D. Gesbert, H. Bölcskei, D.A. Gore, and A.J. Paulraj, "Outdoor MIMO wireless channels: models and performance prediction," *IEEE Trans. on Commun.*, vol. 50, pp. 1926–1934, Dec. 2002.